

Electronic Supplementary Information

For article: *Premelting layer during ice growth: role of clusters*

Shifan Cui^{*a}, Haoxiang Chen^b, Zhengpu Zhao^a

^a*International Center for Quantum Materials, School of Physics, Peking University, 209 Chengfu Road, Haidian District, Beijing 100871, China.*

^b*School of Physics, Peking University, 209 Chengfu Road, Haidian District, Beijing 100871, China.*

Contents

| | |
|--|----|
| 1 Vertical distribution of molecules | 2 |
| 2 Clusters are unstable in small model sizes | 3 |
| 3 Distribution of water and ice in QLL | 4 |
| 4 Cluster evolution is mainly driven by surface diffusion | 5 |
| 5 A simple model on the number density of stable clusters | 6 |
| 6 The stable distribution of clusters lasts long during ice growth | 7 |
| 7 CLC and its relation to region size..... | 8 |
| 8 Relation between IGR and vapor pressure in this work..... | 10 |
| 9 Physics related to clusters are suppressed at lower temperature | 11 |
| 10 Vertical configuration of simulation setup | 12 |
| References..... | 13 |

1 Vertical distribution of molecules

In the "QLL under equilibrium" section of main text we studied the horizontal distribution of molecules in layer 1, and showed the existence of clusters. To further clarify the structure of these clusters, we calculated the vertical distribution of molecules (also in this simulation), at two typical time points: (1) 1 ns, where no clusters have formed; (2) 250 ns, where several large clusters exist. The results are shown in Fig. S1.

Fig. S1(a) shows the vertical molecule distribution profile at two time points, along with the profile of initial structure (perfect crystal) as a comparison. It can be seen that the molecule distribution has almost reached equilibrium after 1 ns, and the shape of the profile agrees with previous studies^{1,2}. However, if we look closely into the region of layer 1 (the inset of Fig. 1(a)), we can notice a significant difference between the profile of two time points (1 ns vs. 250 ns). Namely, the molecule count decays monotonically toward the surface at $t = 1$ ns (orange line), but a peak at ~ 1.2 nm exists at $t = 250$ ns (yellow line). Further analysis shows that this is related to the existence of clusters. Fig. S1(b) explicitly illustrated the vertical profile of layer 1, and decomposed the contribution from clusters and "free" molecules (molecules don't belong to any cluster) for $t = 250$ ns (all molecules are free at $t = 1$ ns). The profile of free molecules is always monotonically decreasing, but a peak exists for the profile of clusters (the "t = 250 ns" graph of Fig. S1(b), orange line). Furthermore, we noticed that the profile of clusters and the equilibrated first bilayer (layer 0) are very similar if we plot them together (bottom graph). This similarity indicates that the clusters actually have the structure of bilayers. Meanwhile, this also means that the clusters are actually "located" in layer 1, and relatively isolated from layer 0 (this can be confirmed by the vertical profile of clusters, which is ~ 0 at the boundary of two layers). Therefore, both the concept of clusters, and the division between two layers, are well-behaved.

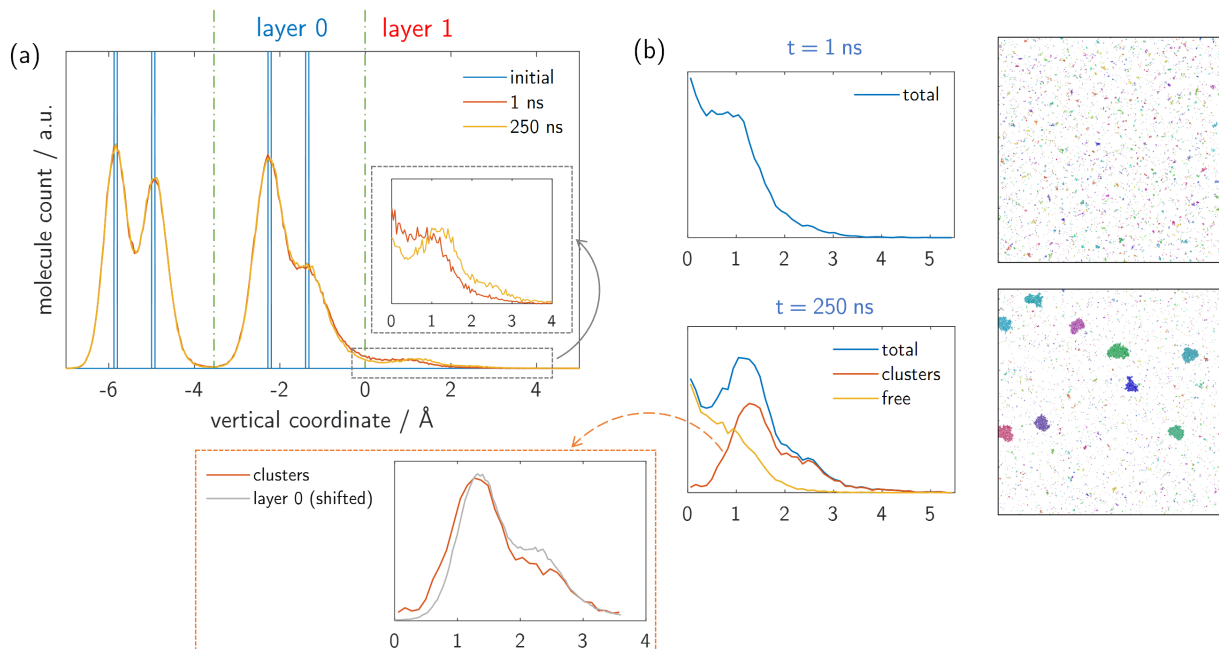


Figure S1. The vertical molecule distribution profile. (a) The vertical profile of initial structure (blue), structure at 1 ns (orange) and 250 ns (yellow), in vertical coordinate range $-7\sim 5$ Å. The zero point of vertical coordinate is the boundary between layer 0 and layer 1. The inset is a magnification of curves in the $0\sim 4$ Å region. The green vertical lines are boundaries of layers. (b) The vertical profile of structure at 1 ns (upper) and 250 ns (lower), in vertical coordinate range $0\sim 5$ Å. The meanings of both axes are same as (a). The horizontal distributions of molecules in layer 1 at two times are shown aside for reference. For decomposing the profile of clusters and free molecules, molecule "groups" with >50 molecules are treated as clusters. The graph at bottom shows the comparison between the profile of clusters (from the 250 ns graph in (b)) and layer 0 (from the 250 ns curve in (a), shifted to draw both curves together).

2 Clusters are unstable in small model sizes

In the “QLL under equilibrium” section of main text we show that small clusters are unstable. In small simulation models, there are not enough molecules in layer 1, prohibiting large clusters to form. The remaining small clusters tend to dissipate quickly, thus are unable to be observed consistently. This is probably the reason why clusters are not reported before.

This argument can be confirmed directly by an MD simulation with a much smaller model (~20 x 20 nm horizontal, ~28000 molecules). All other simulation settings are kept same as the “QLL under equilibrium” section of main text. Results are shown in Fig. S2.

Fig. S2(a) shows the horizontal distribution of molecules in layer 1 at three different times. It is possible to form clusters in such small models, as shown in the middle image ($t = 150$ ns). However, the cluster breaks up later (see the right image, $t = 225$ ns), meaning that such clusters are unstable and cannot be consistently observed. Fig. S2(b) shows the change of largest cluster size during simulation. Some indication of forming clusters can be seen (peaks in the curve), but they are too small (<200 molecules) thus cannot exist for a long time.

It is worth mentioning that, it is still possible to observe stable clusters in small models. As demonstrated in the main text later (and Electronic Supplementary Information (ESI) Section 7), layer concentration (LC) affects cluster formation, and increasing LC will help the formation of clusters in such small models. This can be achieved by adding extra molecules on the surface of initial structure, so more molecules will stay in layer 1 at equilibrium. However, the number of molecules added must be carefully controlled, otherwise clusters may contact each other (or with the periodic mirror of itself).

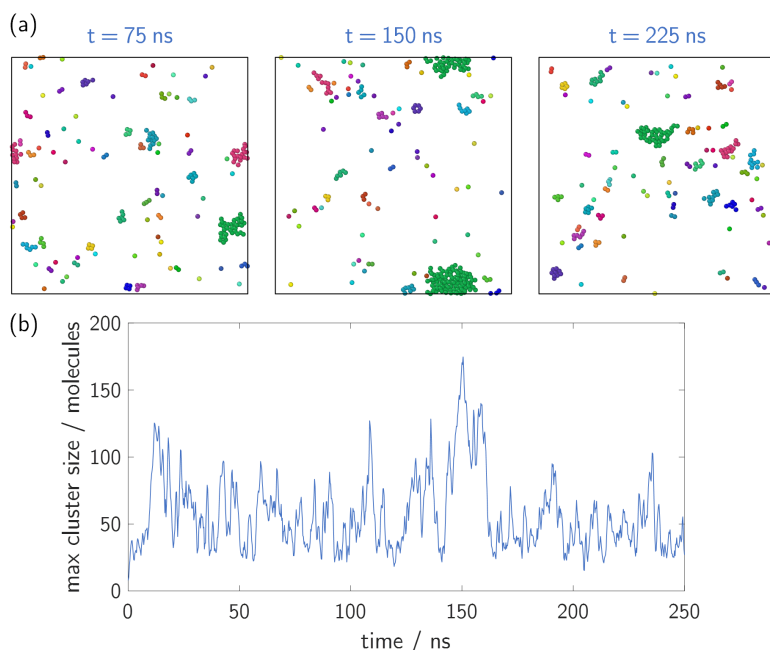


Figure S2. Evolution of clusters in a 20 x 20 nm model. (a) horizontal distribution of molecules in layer 1, at three different times of simulation (75 ns, 150 ns, 225 ns). Molecules are colored by the clusters they belong to. Color choices of different images are not related. (b) maximum cluster size in layer 1 during simulation, as function of time. The curve is slightly smoothed for a better visual appearance.

3 Distribution of water and ice in QLL

Fig. S3 demonstrates the distribution of water (more accurately, molecules with liquid-like structure) and ice (molecules with solid-like structure) in QLL. Fig. S3(a) shows the water-ice distribution of several clusters. They are composed of both water and ice, with stacking faults occurring occasionally. Fig. S3(b) shows the same thing but for the whole layer o , which shows similar behavior as that of clusters. Such a mixed distribution agrees with results in previous study³. However, this is not true for the region in layer o covered by clusters. The shadowed area in Fig. 3(b) shows the location of these clusters, and most of these area is composed of ice (colored yellow/blue) in layer o . That is to say, clusters are mostly “sat” on solid ice rather than liquid water.

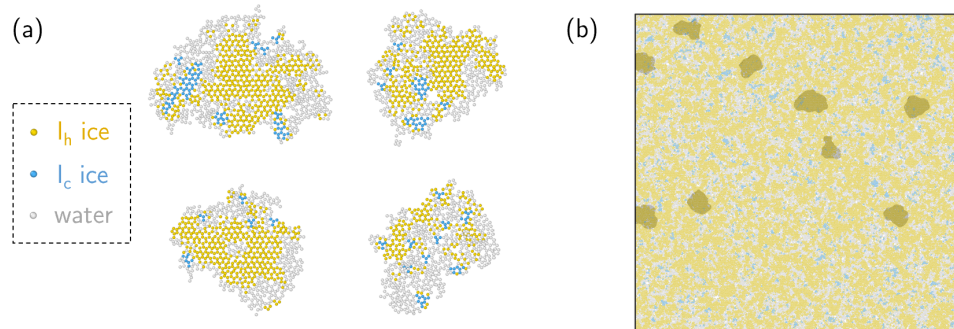


Figure S3. Distribution of water and ice in QLL (clusters & layer o). Hexagonal ice, cubic ice, and water molecules are colored yellow, blue, and grey, respectively (see Computational details section of main text for how they're categorized). The structure is taken from the end of simulation in the "QLL under equilibrium" section of main text ($t = 250$ ns). (a) four typical clusters. (b) layer o as a whole; shadows indicate region covered by clusters (note that clusters themselves are not shown in (b), since they're not in layer o).

4 Cluster evolution is mainly driven by surface diffusion

In the main text we demonstrated the spontaneous formation of clusters, as well as their growth and shrink. In this section we discuss the mechanism behind them.

Theoretically, clusters may form in two mechanisms: (1) gathering of surface molecules by diffusion; or (2) condensed from vapor molecules. To determine the true mechanism, we performed an MD simulation with the same setup as “QLL under equilibrium” section in main text, but with the reflective layer removed. In this setup the ice is effectively sublimating into vacuum, so no condensation from vapor is possible. The horizontal distribution of molecules in layer 1 at several timepoints are shown in Fig. S4(a). Clusters nevertheless form after 100 ns, indicating that vapor condensation is not the major mechanism of cluster formation. In other words, the clusters are mainly formed through molecule gathering by surface diffusion.

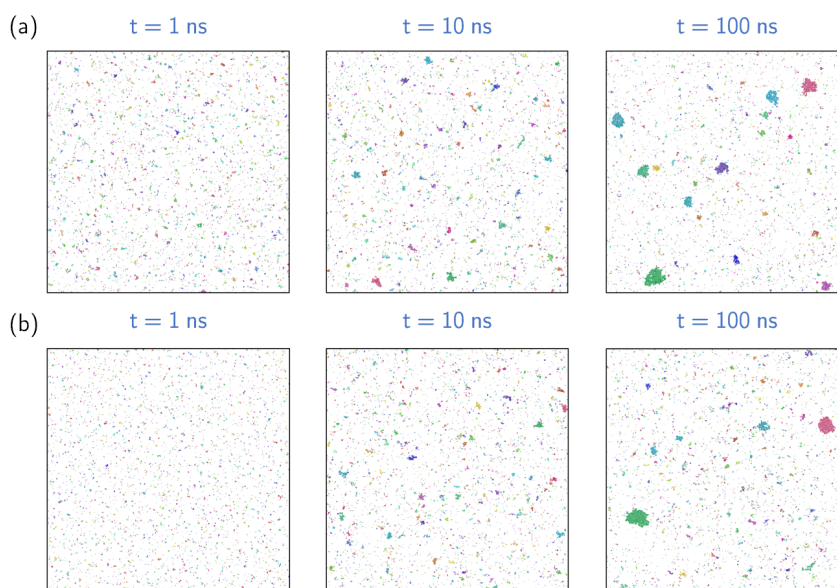


Figure S4. Evolution of QLL under two different conditions. (a) QLL sublimating into vacuum: horizontal distribution of molecules in layer 1, at three different times in simulation. Molecules are colored by the clusters they belong to. Color choices of different images are unrelated. (b) same as (a) but with QLL confined in layer 0 and 1 instead.

Another notable feature in cluster evolution is the shrink of small clusters. Similarly, the shrink could be driven by either surface diffusion, or sublimation of surface molecules. To determine the true mechanism, an MD simulation is performed with a reflective layer placed right at the top of layer 1 (specifically, one bilayer above the boundary between layer 0 and 1). This reflective layer confines the QLL in layer 0 and 1, suppressing all sublimation. The horizontal distribution of molecules in layer 1 under such circumstance is shown in Fig. S4(b). Fewer clusters are found after 100 ns compared to the equilibrium simulation, indicating that the shrinking of clusters is probably enhanced (at least not suppressed). Therefore, the shrinking of clusters is also driven by surface diffusion, rather than sublimation.

Although sublimation and condensation are not direct mechanisms of cluster evolution, they nevertheless affect the dynamics and the final distribution of clusters. This is already shown in Fig. S4, as there're fewer clusters at 100 ns in both simulations than in the equilibrium simulation (compare with Fig. 1(c) in main text). The “QLL during ice growth” section in main text exhibits a more thorough study, showing how the growth rate of ice affects the distribution of clusters.

5 A simple model on the number density of stable clusters

The linear dependence between number density of stable clusters and inverse growth rate (IGR) can be explained by a simple model. First note that molecules in layer 1 can be divided into two types: (1) molecules in clusters, and (2) free molecules (molecules not in any cluster). We will make the following assumptions about these two types of molecules:

- Free molecules move as random walking in layer 1 until they touch any cluster;
- After touching a certain cluster, free molecules will become molecules in that cluster;
- Molecules in clusters always stay in the same cluster.

We will further make the following simplification:

- Area occupied by clusters in layer 1 is small compared to the system size (this is usually true, see ESI Section 6), so (almost) all molecules newly come to the surface are free molecules;
- The growth of clusters is slow (compared to the interval of molecules coming to surface), so the area of “free region” (region not covered by clusters) can be considered as a constant.

Since the amount of clusters does not change, the LC in free region should roughly be a constant (if LC increases to too high, new clusters will form in free region; if LC decreases to too low, existing clusters will dissipate). Since the area of free region is considered constant, the number of free molecules has to be constant. That is to say, the following two rates are equal:

- (1) Rate of new free molecules added;
- (2) Rate of free molecules touching clusters.

(1) is (by simplification) equal to the rate of new molecules coming to the surface, or growth rate. So the inverse of (1) is IGR. The inverse of (2) is the average time required for a free molecule to touch a cluster. Since free molecules are assumed to do random walks, this average time is proportional to d^2 , where d is the average distance between a random point in free region and the nearest cluster. Since clusters are (roughly) uniformly located, d is further proportional to the average distance between clusters. Then $1/d^2$ is proportional to the number of clusters in unit area, so d^2 itself is proportional to inverse number density of clusters. In other words, the inverse of (2) is proportional to the inverse number density of clusters. Since (1) is equal to (2), the inverse number density of clusters is proportional to IGR. The intercept in Fig. 2(c) of main text represents the finite size of clusters, so the number density of clusters cannot be infinite. However, such effect is negligible in realistic scenarios (IGR is very large).

It's necessary to point out that the real world is more complicated. The “mean free path” of free molecules in layer 1 is actually very short, due to frequent exchanges of molecules between layer 0 and layer 1. So the free molecules are not really doing random walks. More likely, the “random walk” of free molecules in layer 1 represents the diffusion of molecules in layer 0, which arguably shows $t \sim d^2$ behavior if traditional diffusion theory is applicable.

6 The stable distribution of clusters lasts long during ice growth

In the “QLL during ice growth” section of main text, we have known about the stable cluster distribution during ice growth. In this section, we will discuss how long does the “stable distribution” hold in the whole process of growth. Here we assume that the ice grows in bilayer-by-bilayer mode (see Fig. 3 of main text; for cluster stacking mode the stable distribution arguably holds at all times). In this mode, the stable distribution establishes when the number of clusters stops changing, and lasts until clusters start to contact each other. Fig. S5(a) shows the horizontal map of molecules in layer 1, right after the establishment of stable distribution. It can be seen that, with IGR increases, the number of molecules in layer 1 at this moment decreases. Fig. S5(b) demonstrates this quantitatively by showing LC corresponding to (a). Therefore, under high IGR in realistic scenarios, the stable distribution starts holding when LC is very low (must <10% and should be way lower). On the other hand, since clusters are (roughly) uniformly located, the LC when clusters start contacting is mostly determined by how they arrange in the 2D plane. In a typical example (simple square arrangement), the LC at this time is $\pi/4 \approx 78.5\%$. Therefore, during the period of growing a full bilayer, the stable distribution holds for $\sim 70\%$ of total time. So we can say the stable cluster distribution dominates the whole process of ice growth.

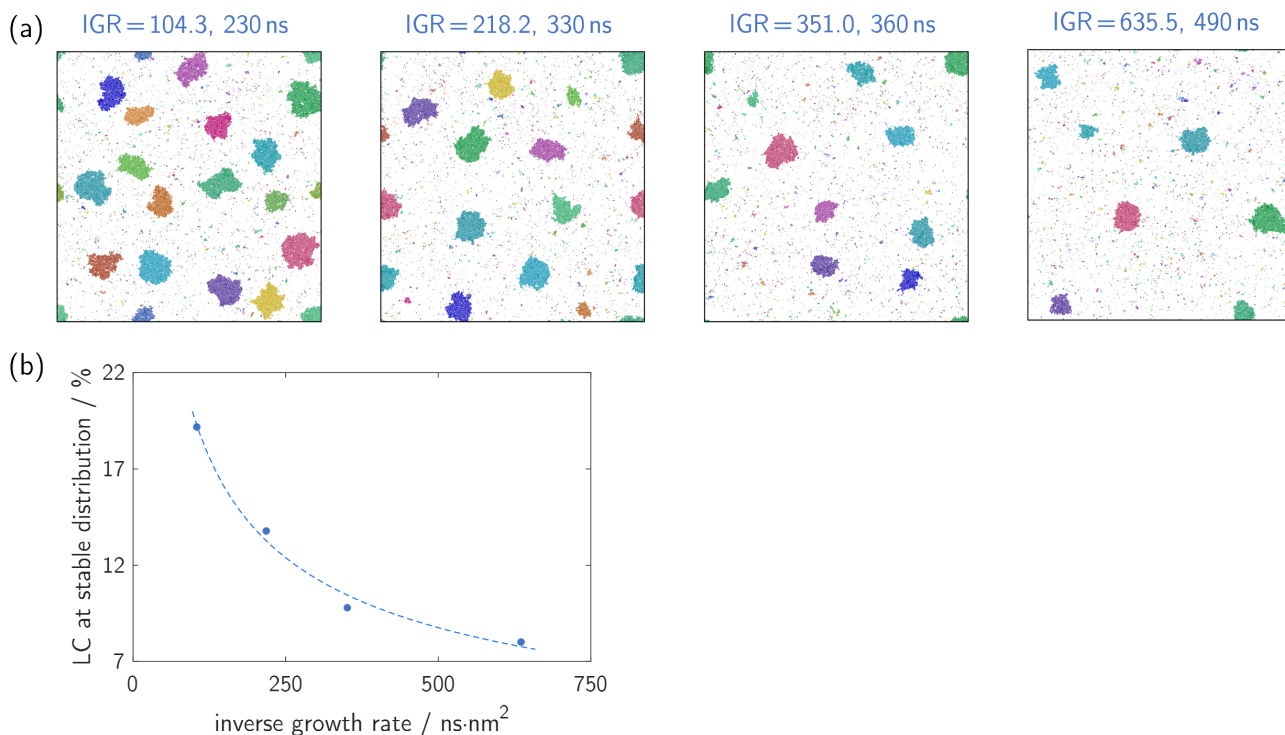


Figure S5. Molecules in layer 1 right after stable distribution is established. (a) horizontal distribution of molecules in layer 1 right after stable distribution established, simulated under four different IGR. The IGR and time corresponding to each image are labeled in the figure (the unit of IGR is $\text{ns}\cdot\text{nm}^2$). Molecules are colored by the clusters they belong to. Color choices of different images are unrelated. (b) The relation between CR (right after stable distribution established) and IGR. Four data points correspond to the four images in (a). The dashed curve serves as a guide to eyes, not a serious fitting.

7 CLC and its relation to region size

In the “growth mechanism of ice” section of main text we claim that high LC prefers cluster formation, and the critical LC (CLC) is a constant unrelated to region size in the thermodynamic limit. However, we don't provide direct evidence there. In this section, we will study the relation between CLC and region size directly by MD simulations.

To this end, we shall first slightly extend the definition of LC. In the main text the region LC defined on is the base cluster. However, it's hard to accurately control the LC on a cluster, and the cluster size continuously changes during ice growth, making quantitative study difficult. Instead, it's more feasible to study the relation between LC and region size in a full-bilayer model under NVT simulations. In such context, we can define LC as the following:

$$LC(M) = \frac{N_{L1}(M)}{A(M) \sigma_{perfect}}$$

where M represents a full-bilayer model, $N_{L1}(M)$ is the number of molecules in layer 1 (red molecules in Fig. 1(a) of main text), and $\sigma_{perfect}$ is same as the one in the main text. The definition here follows the same concept as the one in the main text, except applying for full-bilayer models instead of clusters. Though the boundary of full bilayer models is different from that of clusters, such difference is negligible under thermodynamic limit where the region is very large.

We constructed multiple model systems beginning from perfect I_h ice crystals same as the “QLL under equilibrium” section of main text, but with varied combinations of size and LC (size of 70, 140, 210, and 280 nm; LC varied from 2.9% to 4%, in layer 1). The LC of models are controlled by removing molecules from their surfaces, after an NVT relaxation of 3.75 ns. All models are constructed with no initial clusters to avoid statistical biases, and each with a reflection layer to avoid losing molecules. The simulations are done under NVT ensemble for 150 ns, with the LC and maximum cluster size of each model traced during the whole simulation.

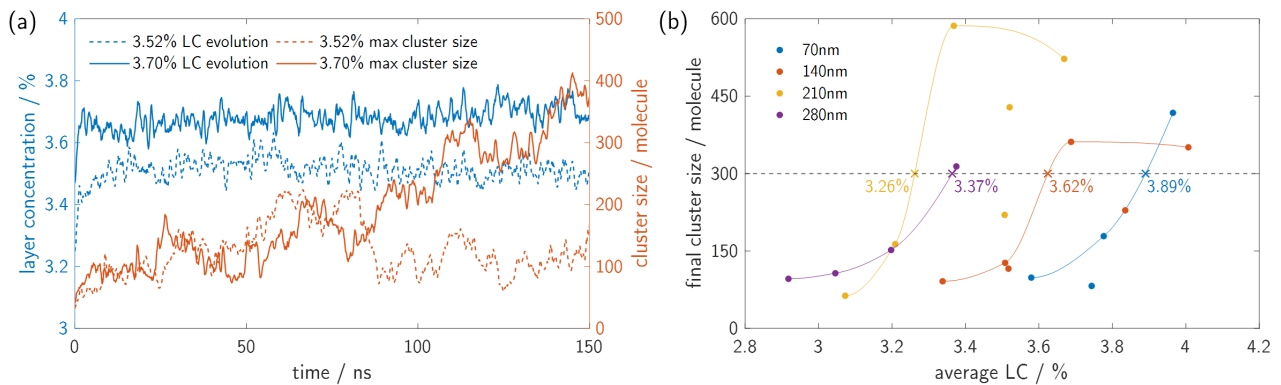


Figure S6. Effect of LC and model size on cluster formation. (a) LC (blue) and maximum cluster size (red) of two typical simulations (average LC of 3.52% and 3.70%, both with the 140 x 140 nm model), as functions of time. See legends in the figure for details. The curves are slightly smoothed for better visual appearance. (b) relation between the final cluster size and average LC. Each independent simulation is represented by a dot, and its color represents the corresponding model size (see legends). Dots with each model size are connected by a curve with the corresponding color. The minimum LC required for forming stable clusters is estimated by the intersection of a curve and the horizontal dashed line (cluster size = 300). Intersections are shown by crosses in the figure, along with corresponding LC labeled. Note that some data points with “too low” final cluster sizes are not considered when connecting curves, because they show lower potential on forming clusters than simulations with lower LC, which is unlikely to be physical (we believe the potential of forming clusters should increase with LC).

Fig. S6(a) shows the temporal evolution of LC and maximum cluster size in two typical simulations. The LC of both simulations keep steady most time, showing that our definition of LC is well-behaved. In the simulation with higher LC (3.70%, solid lines in Fig. S6(a)), the maximum cluster size increases consistently over time, implying

that stable clusters can form under this LC (and model size). In the simulation with lower LC (3.52%, dashed lines in Fig. S6(a)), however, the maximum cluster size goes up only for a while and then goes down again, implying that current LC (and model size) cannot support forming stable clusters. Such observation indicates that high LC favors cluster formation.

Fig. S6(b) shows the results of all simulations in one figure. Each simulation is characterized by two values (along with model size):

- (1) average LC, calculated over last 80% of the simulation;
- (2) final cluster size, averaged over the maximum cluster size of the last 10% simulation. This is the measure of whether stable clusters may form.

Due to the stochastic nature of such simulations (technically “forming clusters” are somewhat rare events), some abnormal behaviors are observed in Fig. S6(b) (e.g. simulation with same model size and higher LC shows lower final cluster size). However, we can still tell that high LC and large system sizes generally favor the formation of clusters.

Now we shall turn to the relation between CLC and region size. In the main text we claim that theoretically the CLC should be a constant when region size reaches thermodynamic limit. More specifically, when the region is sufficiently large (so numerous molecules exist in it), forming a cluster in the layer would only have a marginal effect on the LC of other locations in the layer. That means forming clusters effectively becomes a local behavior (have no effect elsewhere), thus its feasibility only depends on local LC and is irrelevant to the region size. An intuitive analogy for this is the crystallization from solutions, whose feasibility only depends on the concentration of solution and is irrelevant to its volume (as long as it's large enough so crystallization itself has negligible effect on the concentration).

This conclusion is also supported by the MD simulation above. The CLC under each model size can be estimated from results in Fig. S6(b), if we ignore abnormal data points (see footnotes of Fig. S6). Fig. S6(b) shows the estimated CLC for all four model sizes, using 300 molecules as the criterion of forming stable clusters. We found that the CLC is negatively correlated with system size in 70~210 nm, showing that large models can form clusters under lower LC. However, the difference of CLC between 210 nm and 280 nm is small (and the order is “reversed”: the *larger* 280 nm model has a *higher* estimated CLC). The reversed order is likely unphysical, but it also implies that the effect of system size on CLC would be small in large systems (so stochastic factors may dominate), thus supporting our conclusion. This also suggests that the thermodynamic limit is achieved when region size reaches ~210~280 nm, and suggesting a CLC of ~3.3%. In the “growth mechanism of ice” section of main text we used a slightly lower value (3.1~3.3%) for CLC under thermodynamic limit, since such simulations may fail to catch some cluster formation events thus tend to overestimate CLC.

8 Relation between IGR and vapor pressure in this work

In this work we use IGR to describe the growth rate of ice. In real experiments, the growth rate is instead controlled by the vapor pressure of water. However, because the mW model severely underestimates the equilibrium vapor pressure³, we cannot directly compare our results with experiments. This can be more clearly demonstrated if we try to do so, as shown below. For this purpose we make two assumptions:

- (1) water vapor is ideal gas. This is close enough since the vapor pressure is usually much smaller than 1 atm;
- (2) all vapor molecules flying to the surface are absorbed by ice, or the condensation coefficient $\alpha=1$. This is what we observed in our simulations.

After some mathematics, it can be shown that the vapor pressure is given by

$$p = \frac{\pi^{3/2} \sqrt{mk_B T}}{2\sqrt{2} IGR_{add}}$$

where m is the mass of a single water molecule, k_B is Boltzmann constant, T is temperature, and IGR_{add} is the IGR corresponds to molecule addition (i.e. escaped molecules are not subtracted).

As some examples of the formula above, the four simulations in Fig. 2(c) correspond to p of 210, 105, 70, and 42 Pa. For comparison, the equilibrium vapor pressure of water at triple point is ~9 Pa in mW model³, and ~611 Pa in experiment. That saying, the vapor pressure investigated in this work is huge in sense of mW model (as expected), but not even large enough for ice to grow if compared to the real world.

It would be desirable to figure out the source of this incongruity in equilibrium vapor pressure. A noticeable hint comes from the second assumption above: we claimed $\alpha=1$ for ice, but in experiments it's usually found on the level of 0.01~0.1 under similar temperature^{4,5}. This could potentially fill the gap, as a smaller α would require a larger vapor pressure to impose the same molecule addition rate, thus increasing the equilibrium vapor pressure. Further studies on this may focus on accurately calculating the condensation coefficient of mW model, and comparing the results with other water models.

9 Physics related to clusters are suppressed at lower temperature

Most results and discussion in this study focus on a single temperature ($T_m - 0.7K$). In this section, we briefly discuss how temperature could affect results presented in this work. For simplicity we assume no abrupt structural change of QLL with temperature.

As a start point, we shall note that premelting only exists near the melting point; with the temperature decreasing, the phenomena related to premelting are steeply weakened and finally disappear. For demonstration, here we calculated two properties of QLL under two lower temperatures, $T_m - 3.7K$ and $T_m - 8.7K$:

- (1) the molecular ratio of layer 0/layer 1 redistribution (corresponds to Fig. 1(b) in main text);
- (2) the horizontal diffusion coefficient of top two bilayers (specifically, layer 0, the bilayer below layer 0, and layer 1).

For each temperature, an equilibrium simulation of 25 ns in 100 x 100 nm model is performed to calculate these properties. The results are shown in Fig. S7. Significant drops of molecule density in layer 1 (thus LC) are found with temperature decrease (Fig. S7(a)), reducing available molecules for cluster formation. Similar drops exist for diffusion constant (Fig. S7(b)), indicating that the merge of clusters will be slower, so more clusters could coexist in the same area. Combining two factors results in more but smaller clusters. This trend can be demonstrated in an equilibrium simulation, as shown in Fig. S7(c) (compare with the 100 ns snapshot in Fig. 1(c), with only difference in temperature). Such trend weakens the physical meaning of clusters and will finally dismiss it (at low-temperature limit, where diffusion is prohibited and "clusters" will be just single molecules). In that case, the growth of ice is expected to be degenerated into general homogeneous crystal growth from vapor.

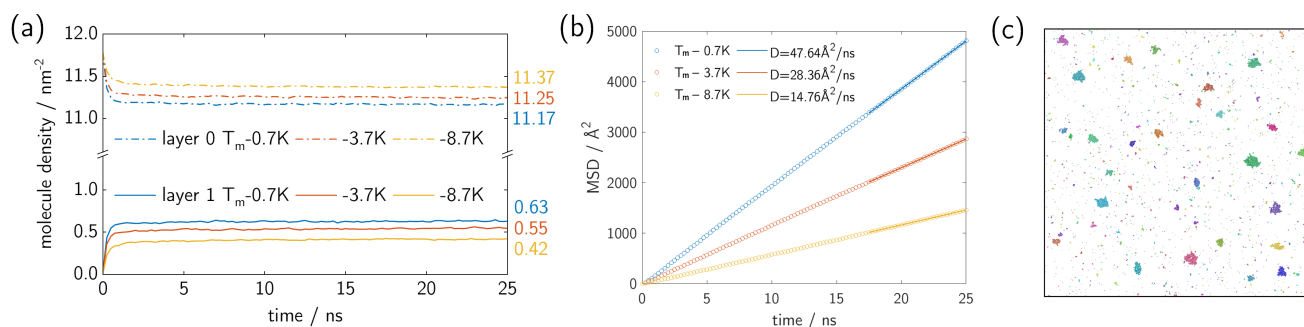


Figure S7. QLL at equilibrium, at three temperatures. (a) molecule density of layer 0 and layer 1, with simulation starting from perfect bilayer. Numbers on the right show the values at 25 ns. The LC of layer 1 at 25 ns are 5.34%, 4.63%, and 3.56% for $T_m - 0.7K$, $-3.7K$, and $-8.7K$, respectively. (b) horizontal mean square displacement (MSD) in first two bilayers (see text above), as well as the diffusion coefficient D (calculated from last 30% of MSD curve). (c) horizontal distribution of molecules in layer 1, at 100 ns of the $T_m - 8.7K$ simulation.

10 Vertical configuration of simulation setup

To observe clusters, simulation models need to have horizontally large scales. However, there are no requirements about the model thickness on the vertical side — as long as it correctly represents surface properties. In the majority of this work, we use a thin model with 4 moveable bilayers and 2 fixed bilayers. Here we discuss the validity of this choice.

To demonstrate this, we shall first notice that the mW model is short-ranged with a 4.32\AA cutoff (that's slightly larger than the thickness of a single bilayer). Meanwhile, the premelting region we are interested in is only ~ 1 bilayer thick (the 2nd bilayer mostly consists of solid³). Therefore, the "omitted" bottom layers would not have a direct impact on the forces felt by premelting molecules. They have indirect effects though, namely by "transmitting" the structure and dynamics across bilayers (e.g. the 4th bilayer has a direct impact on 3rd bilayer, and the structural change of 3rd bilayer further affects 2nd bilayer, etc.). That's saying, the choice vertical configuration should allow the "transmitting" effect to be sufficiently decayed.

To this end, we need to ensure that the properties of QLL would not change much if we alter the vertical configuration. Here we will focus on three properties related to the findings in this paper:

- (1) the molecular ratio of layer 0/layer 1 redistribution;
- (2) the horizontal diffusion coefficient of top two bilayers;
- (3) the ratio of liquid/solid molecules in layer 0.

Apart from the "4 movable + 2 fixed" configuration, two other configurations are considered:

- (1) 6 movable bilayers + 2 fixed bilayers;
- (2) 8 movable bilayers + 0 fixed bilayers (a slab with both surfaces exposed, but we'll only use the upper surface here).

For each configuration, an equilibrium simulation of 25 ns in 100×100 nm model is performed to calculate these properties. The results are shown in Fig. S8. The molecule redistribution between layer 0 and 1 is almost same for all three configurations (Fig. S8(a)), while the diffusion coefficient (Fig. S8(b)) and ratio of liquid molecules (Fig. S8(c)) have differences of 5~10%. Such difference is reasonably small, and much larger error comes from the force field itself. Therefore, adding more layers to the vertical configuration may have some effects on the quantitative results, but it's unlikely to alter main findings of this work.

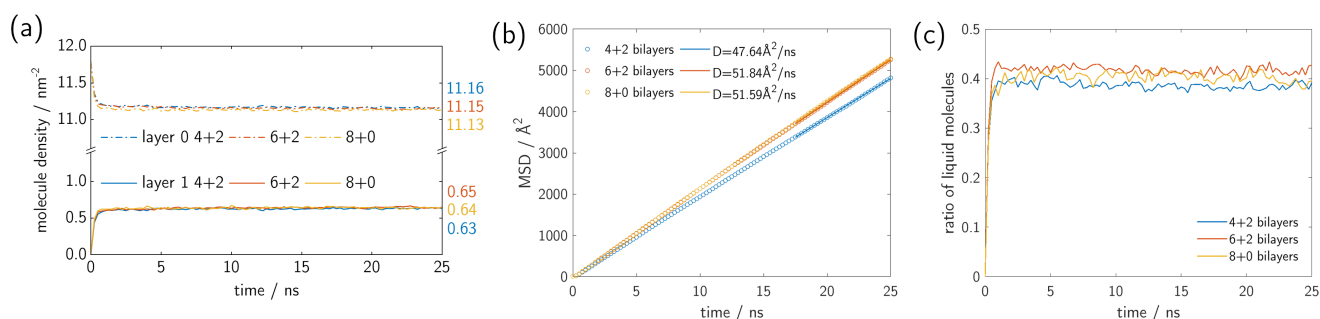


Figure S8. Properties of QLL under various vertical configurations. The "m+n" abbreviation means m movable bilayers and n fixed bilayers. (a) molecule density in layer 0 and 1. (b) horizontal MSD in first two bilayers, as well as the diffusion coefficient D. (c) ratio of liquid molecules in layer 0.

References

1. Bishop, C. L. et al. On thin ice: surface order and disorder during pre-melting. *Faraday Discuss.* **141**, 277-292 (2009).
2. Sánchez, M. A. et al. Experimental and theoretical evidence for bilayer-by-bilayer surface melting of crystalline ice. *Proc. Natl. Acad. Sci. U. S. A.* **114**, 227-232 (2017).
3. Pickering, I., Paleico, M., Sirkin, Y. A. P., Scherlis, D. A. & Factorovich, M. H. Grand Canonical Investigation of the Quasi Liquid Layer of Ice: Is It Liquid? *J. Phys. Chem. B.* **122**, 4880-4890 (2018).
4. Libbrecht, K.G. Explaining the formation of thin ice crystal plates with structure-dependent attachment kinetics. *J. Cryst. Growth.* **258**, 168-175 (2003).
5. Levi, L. & Nasello, O.B. A discussion of mechanisms proposed to explain habit changes of vapor-grown ice crystals. *Atmos. Res.* **66**, 107-122 (2003).